Int J Adv Manuf Technol (2017) 93:3723–3732
DOI 10.1007/s00170-017-0805-0

ORIGINAL ARTICLE

The influence of thermal oxidation and tool-sheet contact conditions on the formability and the surface quality of incrementally formed grade 1 titanium thin sheets

A. Formisano[1] · M. Durante[1] · L. Boccarusso[1] · A. Astarita[1]

Received: 31 January 2017 / Accepted: 12 July 2017 / Published online: 26 July 2017

Abstract The incremental sheet metal forming process combines a series of characteristics, such as the capacity to produce large deformations, flexibility and low-cost tooling, making it preferable to conventional forming processes. One of the key factors in this process are the contact conditions between the forming tool and the sheet to be formed. The incremental forming process of titanium and its alloys is widely studied; on the other hand, the influence of some heat treatments that can induce superficial modifications is not fully known and understood yet. In this study, the influence of thermal oxidation and tool-sheet contact conditions on the formability and the surface quality of grade 1 titanium thin sheets manufactured by incremental forming was investigated by using both a sphere and a hemispherical head tool. The results of the experimental campaign, based on the production of conical and pyramid frusta, highlight the beneficial effects of the heat treatment on the process repeatability, reducing the occurrence of galling for all the contact conditions, and provide information on the quality of the worked surfaces.

Keywords Incremental forming · Titanium · Thermal oxidation · Formability · Surface quality

✉ A. Formisano
aformisa@unina.it

[1] Department of Chemical, Materials and Production Engineering, University of Naples Federico II, Piazzale Tecchio 80, 80125 Naples, Italy

1 Introduction

Titanium and its alloys, despite being considered among the most difficult metals to process [1], are largely used for the production of jet engines, aircrafts components, sporting goods and surgical instruments, thanks to their properties of biological inertness, high specific strength, corrosion resistance and light weight [2, 3].

Given the request of customised production in a wide range of applications and relatively to the sheet metal forming techniques, the interest for the incremental forming in all its variants [4] is growing, due to its flexibility and ability to respond quickly to market demands. The basis of this class of forming processes is the imposition of localised deformations to a peripherally clamped sheet by using a tool, typically with hemispherical head, describing a path controlled through a CNC machine [5].

The tool-sheet contact is an important issue in the incremental forming of titanium and its alloys that are characterised by poor tribological properties [6–8], including high and unstable friction coefficient, severe adhesive wear, susceptibility to fretting wear, scuffing and a strong tendency to seize [9]. These poor tribological properties are due to its electron configuration, crystal structure and lubrication conditions [6]. However, the tribological properties of titanium and its alloys can be changed by means of surface treatments promoting the growth of an adherent and harder oxide layer on the surface, leading to a change of the wear mechanism and to a lowering of the wear rate [10].

Many methods were adopted to produce the abovementioned oxide layer on the Ti surface [11] such as anodising [12–14], ion implementation [15, 16], oxygen diffusion [17], palladium-treated thermal oxidation [18] and thermal oxidation [19, 20]. The thickening of the passive layer through the application of thermal oxidation (TO) is a simple and cheap

method of modifying the surface of titanium and its alloys [21]. The so-modified surface shows better properties than the ones modified by others methods [11]. Moreover, this is a treatment capable to enhance the wear resistance of titanium alloys by inducing the formation of a thick, highly crystalline, tough and hard rutile oxide layer (TiO_2) [6, 22, 23]. As a rule, such an oxide layer is poorly bonded to the substrate [24, 25]; nevertheless, its hardening effect is sufficient to enhance the wear resistance of titanium alloys [6, 12, 21–25].

Furthermore, thanks to this treatment, a change in the wear mechanism was also observed [26]; in particular, the occurrence of galling was avoided. The galling is a type of adhesive wear caused by macroscopic transfer of material between metallic surfaces during relative sliding motion that can generate scratches on the worked surfaces. This phenomenon constitutes a very relevant problem in the sheet metal forming industry [27, 28] that mostly affects the titanium alloys [29].

In this study, the material investigated is the unalloyed titanium, grade 1 that is mainly used for airframes, aircraft engines, marine chemical components, heat exchangers, condenser and evaporator tubing and shows good formability, ductility, weldability and corrosion resistance [30].

In a previous paper on the incremental forming of this material, it was stated that the most relevant aspect is that only the sphere as tool guarantees a good process repeatability [31]; for the severest tool-sheet contact conditions, the formability decreases as effect of the galling phenomenon. Moreover, the effect of stress-relieving heat treatment on the surface topography and the dimensional accuracy of parts formed by incremental forming was also investigated [32]. These studies were carried out on untreated sheets; the influence of a superficial treatment on the forming behaviour of titanium alloys is to date, to the authors best knowledge, not fully known and understood.

Aiming to fill this lack of knowledge, in this study, the influence of the TO treatment on the incremental forming process of grade 1 titanium sheets was investigated. This treatment, as previously discussed, changes the sheets surface properties and, consequently, the tool-sheet contact conditions. To this scope, both treated and untreated grade 1 titanium thin sheets were incrementally formed under three different tool-sheet contact conditions, by using as forming tools (i) a sphere, (ii) a fixed hemispherical head and (iii) a rotating hemispherical head.

The formability angles were evaluated through the varying wall angle conical frusta (VWACF) tests [33]; instead, scanning electron microscope (SEM) observations and the analysis of the forming forces and of the main roughness parameters were carried out on pyramid frusta specimens with a fixed wall angle. The last analyses supported the results of the formability tests and provide useful indications on the surface quality.

Table 1 Chemical composition of titanium grade 1 (AMS 4901T SAE standard)

Element	% in weight
Carbon	<0.10
Hydrogen	<0.015
Iron	<0.30
Nitrogen	<0.030
Other, total	<0.30
Oxygen	<0.25
Titanium	99.2

2 Materials and methods

Titanium grade 1 rolled sheets, 0.66-mm thick, were used in this experimentation; the chemical composition and the main mechanical properties of this material are reported in Tables 1 and 2, respectively.

Following as done by the authors in a previous paper [26], the TO treatment was carried out in a warm air furnace, under atmospheric pressure and at a temperature of 650 °C for 6 h, in order to obtain the desired rutile layer. After the exposure at high temperature, the samples were allowed to cool in the furnace for about 10 h.

Aiming to evaluate the influence of the TO treatment, detailed metallographic observations were carried out on both untreated and heat-treated sheets, by using a Hitachi TM 3000 SEM equipped with an EDX microanalysis probe. Moreover, micro Vickers hardness tests, aiming to highlight the hardness increase due to the heat treatment, were carried out according to ASTM E384 standard on specimens cut from both untreated and treated sheets; at least five valid measurements were obtained for each specimen, setting an indentation load of 100 g and a loading time of 20 s.

Both conical frusta with an arc of circle as a generatrix and pyramid frusta were manufactured by incremental forming; the equipment used during the tests is reported in Fig. 1. On the basis of previous papers [34, 35], in which it was proved that the temperature influences the softening of the material to be formed but not its forming behaviour, it was chosen to carry out the forming process at room temperature. The geometrical features of the profiles are reported in Fig. 2: concerning the conical frusta (Fig. 2a), R_g is the generatrix radius, D_{MAX} the maximum

Table 2 Mechanical properties of titanium grade 1 (AMS 4901T SAE standard)

Hardness, Brinell	200
Ultimate tensile stress (MPa)	430
Yield strength (MPa)	340
Young modulus (GPa)	102
Elongation at break (%)	28

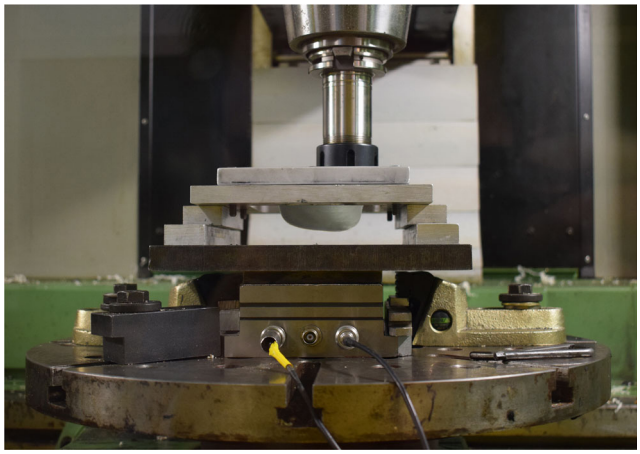

Fig. 1 Equipment for the incremental forming tests

diameter and α_0 the initial wall angle; regarding the pyramid frusta (Fig. 2b), L_{MAX} is the side of the major base, α the wall angle and h the height. The previously defined features are given in Table 3.

The clamping system of the sheets has a square forming area, 100 mm × 100 mm; the forming tests were carried out by a C.B. Ferrari high-speed four-axis vertical machining centre. Spiral tool paths were described in anticlockwise direction, and a feed of 3000 mm/min was set. For the cones, an angular step of 1° was set, whereas for the pyramids, two different vertical steps were chosen: 0.5 and 1 mm.

Different tool-sheet contact conditions were investigated, as stated in Sect. 1, by using as tools a sphere and a cylindrical punch with hemispherical head, both made of steel and with a radius of 5 mm. Moreover, the punch was tested both in unrotating and in rotating conditions, at an anticlockwise rotational speed of 500 rpm. Such a decision, i.e. to use a steel tool, was done on the basis of a previous work of the authors [36], in which the contact between a steel tool and both treated and untreated titanium sheets was studied and it was pointed out that the occurrence of the galling was avoided when the titanium sheets were properly treated. During the forming tests, the sheets to be formed were lubricated with a thin layer of oil to reduce the friction and, thus, the risk of failure.

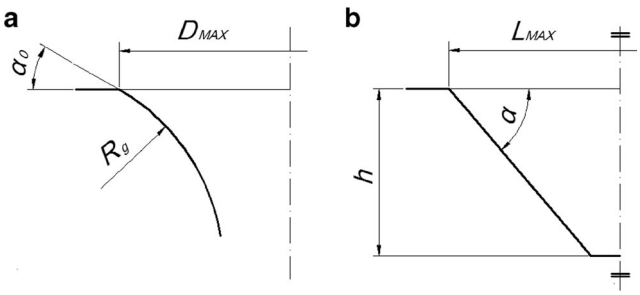

Fig. 2 Features of the profiles for conical (**a**) and pyramid frusta (**b**)

Table 3 Values of the geometrical features of the profiles

R_g (mm)	D_{MAX} (mm)	α_0 (°)	L_{MAX} (mm)	h (mm)	α (°)
50	80	30	80	39	50

The formability angles were evaluated by means of the VWACF tests; five tests were carried out for each case study. The tests were stopped when the failure occurred and the crack, together with the tool path advancement, propagated circumferentially; the formability angles were evaluated in correspondence with the failure, so as illustrated in Fig. 3.

Therefore, further considerations based on the interpretation of the forming forces and on the analysis of the formed surfaces of the pyramid frusta were done.

Relatively to the forming forces, the clamping system of the sheets is rigidly fixed to the upper plane of a Kistler load cell, in order to measure two components of the reaction forces of the sheets (F_z and F_y). Of each square spiral of the tool path, only two tracts were considered, since the other two show substantially the same absolute force values, but with opposite sign. Figure 4 schematises the forming process with the correct orientation of the forces components and highlights the two tracts (the arrow indicates the tool path direction): the first one (*a*), in which the sheet reacts to the friction by the tool-sheet relative motion and the flattening of the feed rate; the second one (*b*), in which the contribution linked to the thrust on the faces of the pyramid frustum prevails [37].

In order to study the phenomena occurring on the sheets during the forming process under the different contact conditions, the surface of the sheets after the forming process was observed through the SEM microscope.

Finally, a quantitative surface analysis was carried out through the evaluation of three linear roughness parameters, i.e. the mean roughness (R_a), the root mean square roughness (R_q) and the mean roughness depth (R_z), and a hybrid areal roughness parameter, i.e. the developed interfacial area ratio (*Sdr*). This last parameter is defined as the percentage of additional surface area contributed by the texture as compared to an ideal plane (the sampling area) and may further

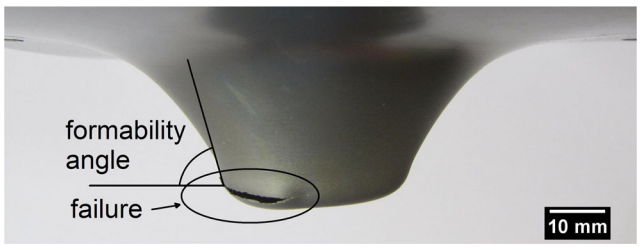

Fig. 3 Formability angle by VWACF tests

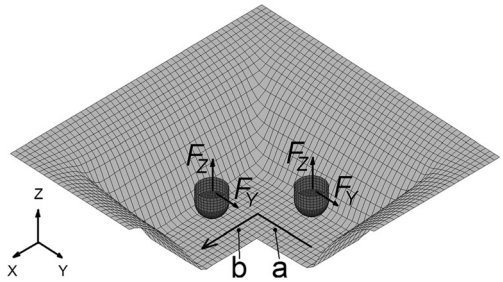

Fig. 4 Schematisation of a forming process with the forces components

differentiate surfaces of similar amplitudes and mean roughness. Therefore, the *Sdr* indicates the complexity of a surface thanks to the comparison of the curvilinear surface and the support surface. A completely flat surface will have a *Sdr* equal to 0%, instead of a complex surface that will have a *Sdr* of some percents. The linear parameters were measured perpendicular to the direction of the tool movement, by means of a rugosimeter Surftest SJ-301 with differential inductance used as the detecting method and with Gaussian filter. Measures with different cut-off values, 0.8 and 2.5 mm, were carried out according to ISO 4288-1996 standard relatively to the recommended cut-off values. Ten measures were recorded for each case, divided equally over two contiguous internal faces of the pyramid frusta to avoid casual errors linked to any anisotropic behaviour in terms of sheet roughness. The areal parameter was measured by means of a confocal microscope Leica DCM 3D with a magnification of ×10 on a sampling area equal to 5.0 × 5.0 mm, according to ISO 25178.

3 Results

With regard to the influence of the TO treatment on the undeformed sheets, the surfaces of the untreated and heat-treated sheets, obtained by SEM, are given in Fig. 5. Moreover, from micro Vickers hardness tests, mean values of 164.0 and 200.4 were evaluated for untreated and treated sheets, respectively, with standard deviations of 2.5 and 8.2.

Table 4 Formability angles by VWACF tests

Treatment	Tool	Formability angle (°)
Untreated	Sphere	71.16 (0.67)
	Hemispherical head—0 rpm	65.18 (3.16)
	Hemispherical head—500 rpm	65.16 (4.36)
Treated	Sphere	71.08 (0.81)
	Hemispherical head—0 rpm	67.32 (1.02)
	Hemispherical head—500 rpm	67.38 (0.98)

Relatively to the formability, Table 4 reports the formability angles, both in terms of mean and standard deviation values (reported between round brackets), obtained by VWACF tests.

Regarding the remaining analyses, pyramid frusta were manufactured by using both the sphere and the hemispherical head tool, but only in unrotating conditions; in fact, the rotating tool was not considered yet, due to the very low surface quality reached with this contact condition.

The process was successfully completed for all the cases, even if the frustum formed under the severest conditions (i.e. using an untreated sheet, the hemispherical head tool and a vertical step of 1 mm) shows failures that occur at the corners, that is the most stressed zones [38], and they propagate along the edges (Fig. 6).

For each case, the ratio F_y/F_z was considered; Fig. 7 reports an interval of the steady-state curves after an increasing initial phase.

Relatively to the surface analysis, Fig. 8 reports SEM observations of the pyramid frustum surfaces for all the four different conditions; moreover, the values of the investigated roughness parameters are reported in the histograms of Figs. 9 and 10 (for the linear ones, both in terms of mean value and standard deviation). Table 5 summarises the specimens' IDs

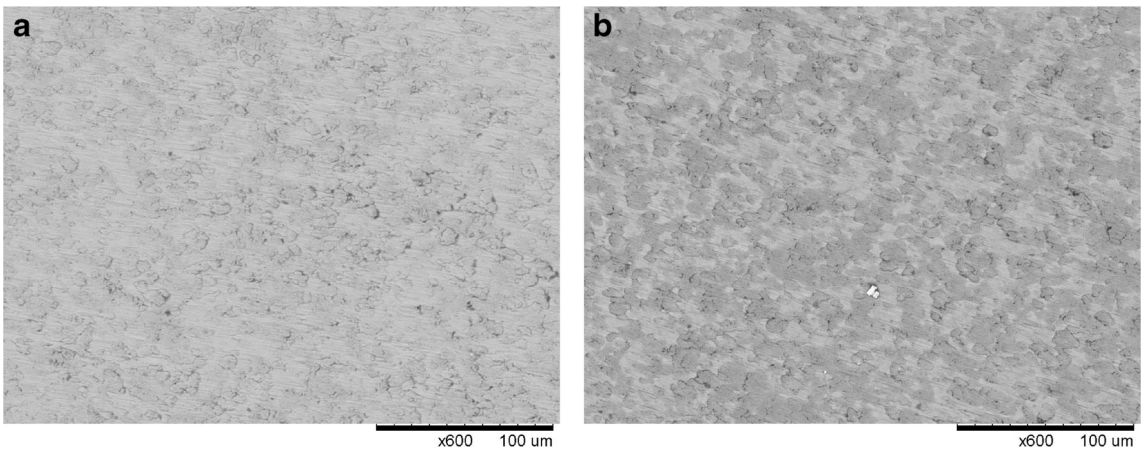

Fig. 5 SEM images of the top surface of untreated (**a**) and heat-treated undeformed sheets (**b**)

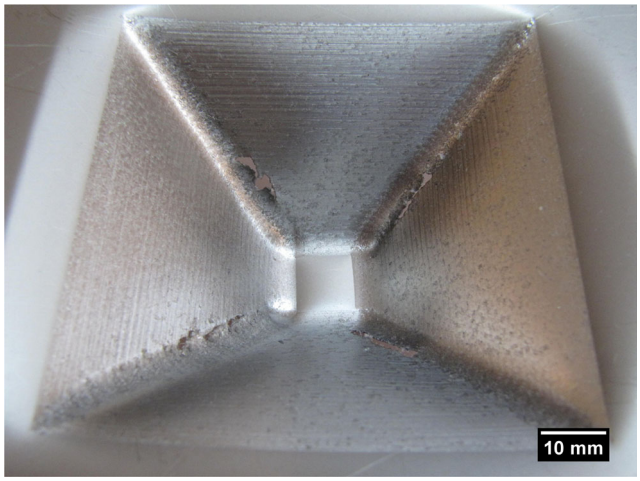

Fig. 6 Fractures along the edges of a conical frustum (untreated sheet, hemispherical head tool, vertical step of 1 mm)

reported as abscissas of the histograms (S0t and S0u are related to treated and untreated undeformed sheets).

4 Discussion

As can be observed from the images of Fig. 5, the heat treatment changes the superficial microgeometry of the sheets. The TO treatment causes the formation of an oxide layer on the top surface of the sheet, confirmed by the EDX spectra of Fig. 11; this layer is harder than the base material, as highlighted by the results of the microhardness tests.

Analysing the values of formability (Table 4), it is evident that the heat treatment provides beneficial effects in terms of process repeatability, not only by using the sphere; in fact, the standard deviation of the formability angles results to be very lower than the untreated sheets. In particular, when using the hemispherical head tools, the heat-treated sheets do not show localised failures that, conversely, for the untreated ones can occur before reaching the maximum values of the formability (Fig. 12, tool rotating); this can determine a premature failure of the sheets and, consequently, the higher variability highlighted by the standard deviation. Nevertheless, the

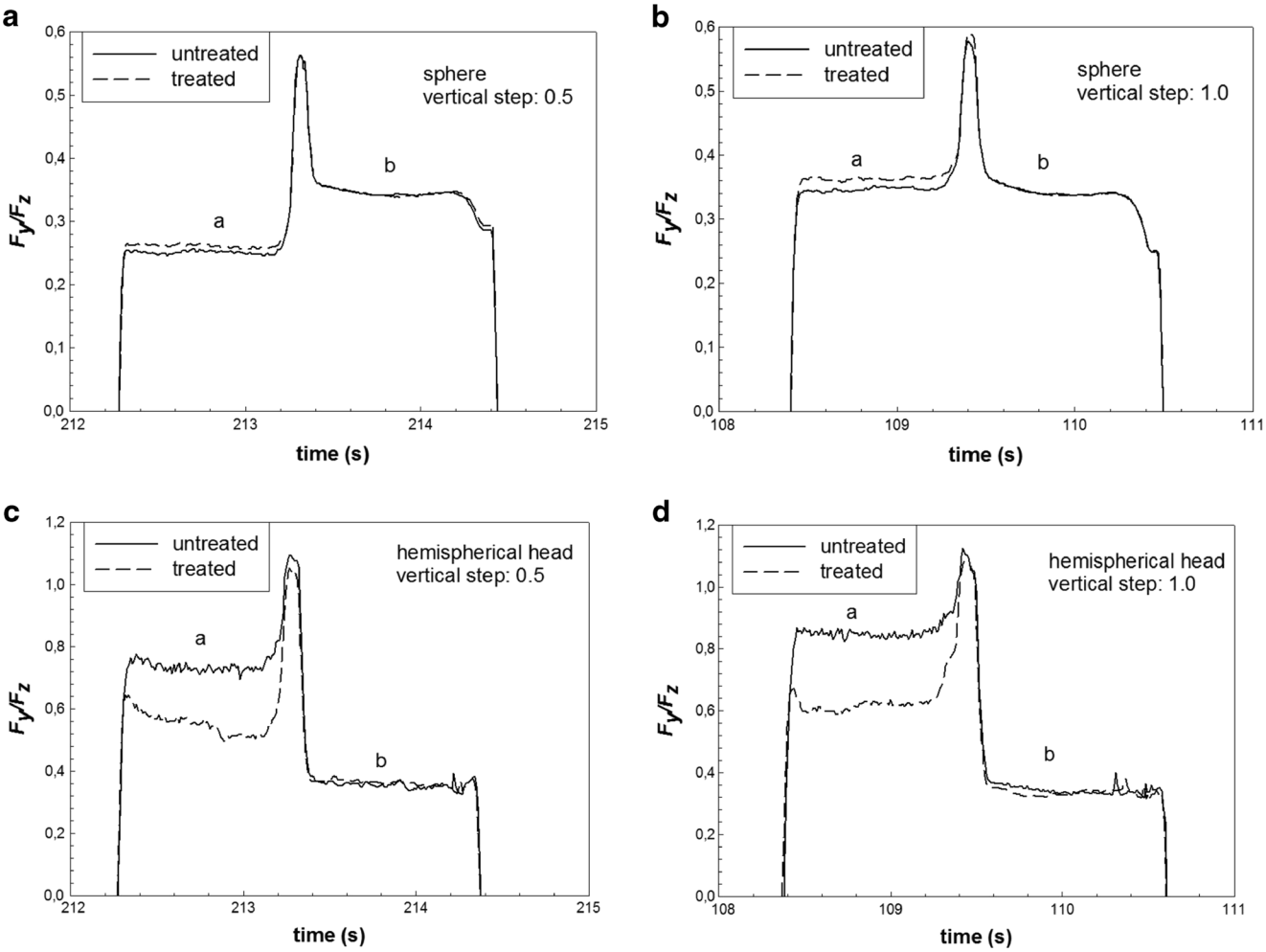

Fig. 7 Ratio between the horizontal and the vertical force components by incremental forming of pyramid frusta for: sphere, vertical step of 0.5 mm (**a**); sphere, vertical step of 1 mm (**b**); hemispherical head tool unrotating, vertical step of 0.5 mm (**c**); hemispherical head tool unrotating, vertical step of 1 mm (**d**)

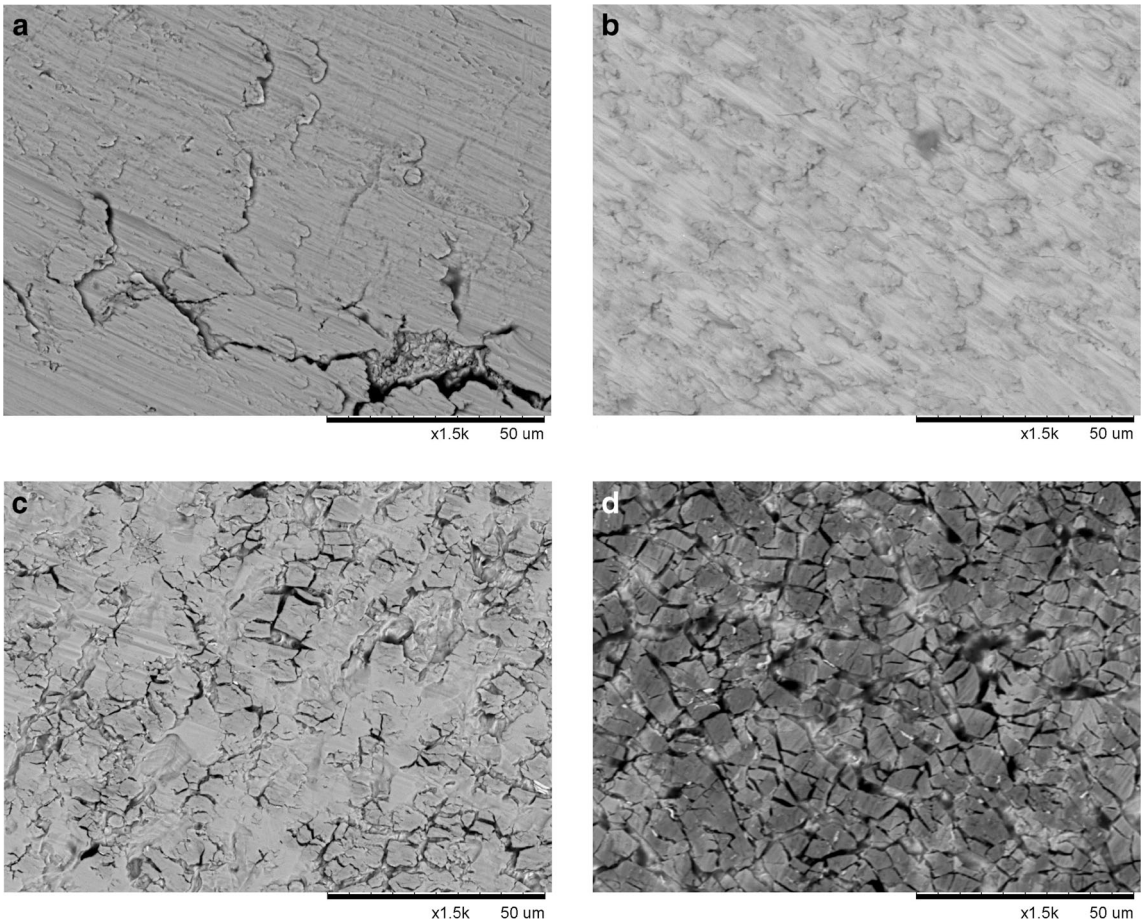

Fig. 8 SEM images of the worked surface for untreated sheet, hemispherical head tool unrotating (**a**); heat-treated sheet, hemispherical head tool unrotating (**b**); untreated sheet, sphere (**c**); and heat-treated sheet, sphere (**d**)

phenomenon of galling also occurs for the treated sheets, especially when the rotating tool was used, as shown in Fig. 13. However, it does not involve any premature failures of the specimen and, then, it does not affect the formability.

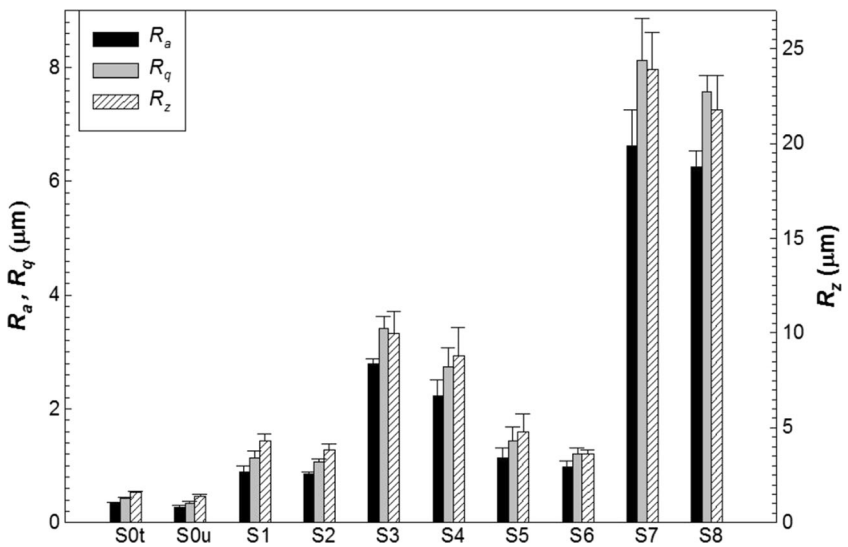

Fig. 9 Values of linear roughness parameters

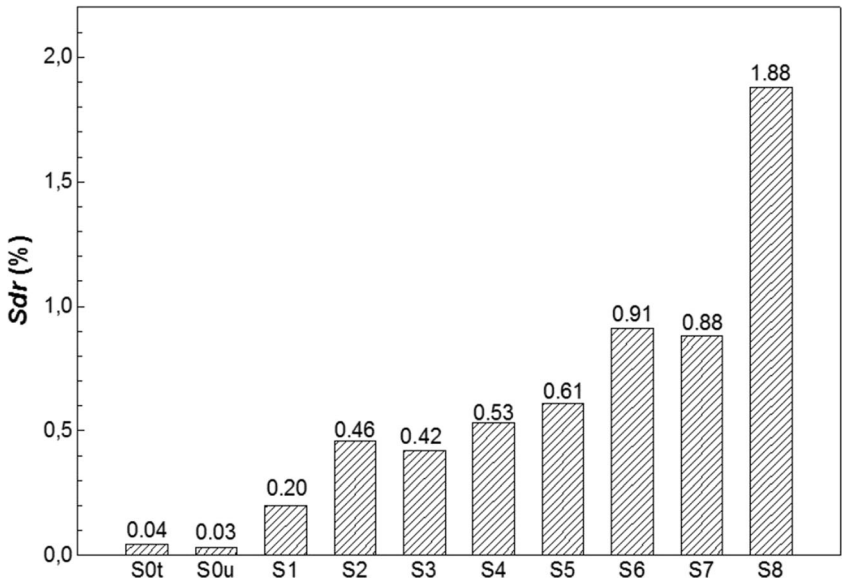

Fig. 10 Values of areal roughness parameter

Finally, the mean values of formability angles highlight the goodness of using the sphere, in keeping with the results of a study on the sheet incremental forming of four grades of aluminum alloys [39].

Passing to the analysis of F_y/F_z trends (Fig. 7), they show a peak when the tool reaches the corner of the path, between the tracts *a* and *b*. It is possible to highlight that

- the values for the tract *b* are almost equal for all the cases (0.35); then, they do not depend on the contact conditions, the vertical step and the heat treatment but only depend on the wall angle of the obtained geometry.
- the heat treatment is almost irrelevant on the tract *a* when the sphere is used. In fact, the curves overlap for both vertical steps (Fig. 7a, b) and assume a higher value as the step increases (about 0.25 against about 0.35); this is a consequence of the higher flattening at which the sheet is subject. The observations in these two ultimate bulleted points confirm what previously anticipated [37].
- both the untreated and heat-treated sheets are subject to galling when the tool with hemispherical head is used (Fig. 7c, d); in fact, the curves result more jagged as a consequence of the scratching. In addition, F_y/F_z values are very higher, compared to the sphere, due to the increase of friction, for the tract *a*; relatively to this, the figures highlight the influence of the treatment, since the treated sheets show the lowest value, compared to the untreated ones.

Relatively to the surface quality, galling phenomenon can be observed for both treated and untreated sheets formed by the hemispherical head tool (Fig. 8a, b). The severity of the galling is different; in particular, the untreated sheets show a much more severe galling wear (Fig. 8a) with respect to the heat-treated ones (Fig. 8b). This result is also in agreement with the measured forces: in fact, looking at the diagrams presented in Fig. 7c, d, it is possible to note a higher frictional force for the untreated sheets. In this case, the treatment, by promoting the growth of a harder oxide layer, causes a change in the contact conditions, with a reduction of the severity of the galling phenomenon as previously said and as proved by the presented images. SEM images of the surfaces formed by the sphere reveal a completely different superficial morphology (Fig. 8c, d). In this case, the contact conditions are completely different and as first result, by observing the previously reported

Table 5 Identification of the specimens for the interpretation of the roughness results

Specimen ID	Sheet	Tool	Vertical step (mm)
S0t	Treated	–	–
S0u	Untreated	–	–
S1	Treated	Sphere	0.5
S2	Untreated	Sphere	0.5
S3	Treated	Hemispherical head	0.5
S4	Untreated	Hemispherical head	0.5
S5	Treated	Sphere	1.0
S6	Untreated	Sphere	1.0
S7	Treated	Hemispherical head	1.0
S8	Untreated	Hemispherical head	1.0

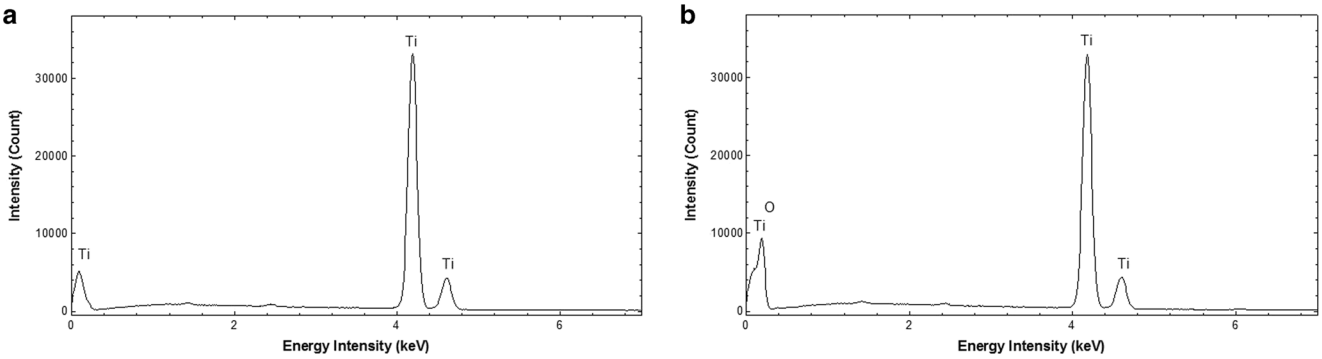

Fig. 11 EDX spectra of untreated (**a**) and heat-treated undeformed sheets (**b**)

images, it is possible to affirm that the galling phenomenon does not occur for both treated and untreated sheets. Once again, this result is in agreement with the measured forces (Fig. 7a, b); indeed, the frictional forces measured when the sphere was the forming tool are much lower than the ones measured when the hemispherical tool was used. In this case, i.e. spherical tool, the surface appears cracked for both treated and untreated sheets. The TO treatment seems to promote the occurring of these cracks; as a matter of fact, the treated surface appears much more cracked (Fig. 8d) than the untreated one (Fig. 8c). Such is a result, because the TO leads to the formation of an oxide layer that is brittle; so when the bulk material experiences plastic deformation, the oxide layer (that behaves as a ceramic material) is not able to follow the same deformation entity involving in the formation of the cracks. Concerning the untreated material, the natural oxide layer is less brittle, so there is a reduced formation of cracks. It is important to point out that these cracks are appreciable only at high magnification; the macroscopic appearance of the surfaces is good in both the cases.

In Fig. 9, it is possible to highlight that the roughness increases with the vertical step, especially using the hemispherical head tool. Moreover, the sphere guarantees a quality of the worked surfaces almost comparable to the one of the undeformed sheets; in particular, an almost regular profile, in which only the technological signatures due to the tool-sheet contact occur, characterises the surface obtained by the sphere (Fig. 14a, b). Conversely, the tool with hemispherical head causes an increase of roughness; this contact condition generates a scratched surface, consequent to the overlay of abraded material with the technological signatures (Fig. 14c, d). Nevertheless, in all the cases, the R_a values are included in the category of the surfaces obtained by machining or hand grinding, according to ISO 4287/1.

Relatively to the influence of the heat treatment, it is substantially uninfluential when using the sphere, whereas with the hemispherical head tool, the roughness is always slightly higher for the treated sheets. This can be due to the action of the tool on the abraded material, as a consequence of galling; this smearing effect is more significant on the untreated sheets (as also highlighted by the higher values of the forces for the tract *a* in Fig. 7c, d), since their surface shows lower hardness, compared to the treated ones, and this reduces the roughness. Nevertheless, the untreated sheets show a greater surface irregularity, as highlighted by the higher values of *Sdr* (Fig. 10).

Summarising the previously discussed results, both the forming tool and the treatment deeply influence the forming process; the best results are obtained with the sphere as forming tool and with heat-treated sheets. The combination of treatment conditions and forming tool used determines the contact conditions and the final appearance of the formed surfaces.

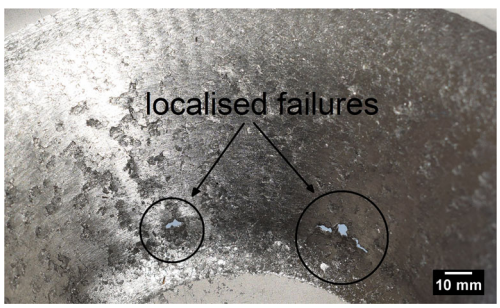

Fig. 12 Localised failures on untreated sheet formed by hemispherical head tool rotating

Fig. 13 Scratched sheet, heat-treated, formed by hemispherical head tool rotating

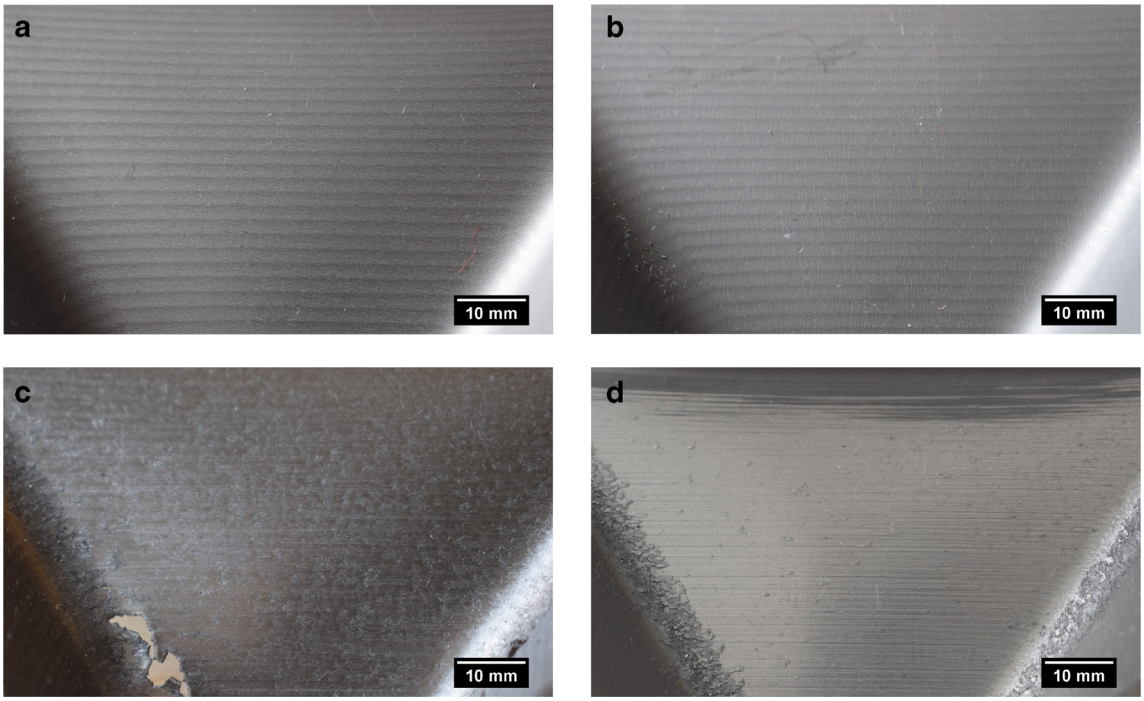

Fig. 14 Worked surface for untreated sheet, sphere (**a**); heat-treated sheet, sphere (**b**); untreated sheet, hemispherical head tool unrotating (**c**); and heat-treated sheet, hemispherical head tool unrotating (**d**)

In a future work, it will be interesting to find which is the maximum deformation of the sheets that can be achieved without cracking the oxide layer.

5 Conclusions

This study compares untreated and thermally oxidised incrementally formed grade 1 titanium thin sheets, in terms of formability and surface quality, by using a sphere and a cylindrical tool with hemispherical head, both rotating and unrotating. The main results can be summarised as follows:

- the thermal oxidation treatment induces the formation of a harder oxide layer on their surfaces;
- the maximum formability angle from varying wall angle conical frustum tests reaches a value of about 71.2° when using the sphere on untreated sheets;
- the process repeatability, in terms of formability, is guaranteed for the heat-treated sheets under all the investigated tool-sheet contact conditions;
- the process effectiveness is worse for the untreated sheets, despite their lubrication, when the sphere is not used, because of the occurring of the galling. This wear phenomenon also occurs, but for smaller scale, on the heat-treated sheets;
- the thermal oxidation treatment has a slight influence on the linear roughness, whereas guarantees higher regularity of the worked surfaces, since it preserves them from galling.

References

1. Semiatin SL, Seetharaman V, Weiss I (1997) The thermomechanical processing of alpha/beta titanium alloys. J Miner Met Mater Soc 49(6):33–39. doi:10.1007/BF02914711
2. Krebs RE (2006) The history and use of our earth's chemical elements: a reference guide, 2nd edn. Greenwood Publishing Group
3. Bannon BP, Mild EE (1983) Titanium alloys for biomaterial application: an overview. In: titanium alloys in surgical implants. ASTM STP 796:7–15
4. Emmens WC, Sebastiani G, van den Boogard AH (2010) The technology of incremental sheet forming—a brief review of the history. J Mater Process Tech 210(8):981–997. doi:10.1016/j.jmatprotec.2010.02.014
5. Behera AK, Lauwers B, Duflou JR (2015) Tool path generation for single point incremental forming using intelligent sequencing and multi-step mesh morphing techniques. Int J Mater Form 8(4):517–532. doi:10.1007/s12289-014-1174-y
6. Dong H, Bell T (2000) Enhanced wear resistance of titanium surfaces by a new thermal oxidation treatment. Wear 238(2):131–137. doi:10.1016/S0043-1648(99)00359-2
7. Miller PD, Holladay JW (1958) Friction and wear properties of titanium. Wear 2(2):133–140. doi:10.1016/0043-1648(58)90428-9
8. Budinski KG (1991) Tribological properties of titanium alloys. Wear 151(2):203–217. doi:10.1016/0043-1648(91)90249-T
9. Blau PJ (1992) ASM handbook volume 18: friction, lubrication, and wear technology. ASM International
10. Bloyce A, Morton PH, Bell T (1994) ASM handbook volume 5. ASM International

11. Aniołek K, Kupka M, Barylski A (2016) Sliding wear resistance of oxide layers formed on a titanium surface during thermal oxidation. Wear 356-357:23–29. doi:10.1016/j.wear.2016.03.007
12. Siva Rama Krishna D, Brama YL, Sun Y (2007) Thick rutile layer on titanium for tribological applications. Tribol Int 40(2):329–334. doi:10.1016/j.triboint.2005.08.004
13. Cui X, Kim H-M, Kawashita M, Wang L, Xiong T, Kokubo T, Nakamura T (2009) Preparation of bioactive titania films on titanium metal via anodic oxidation. Dent Mater 25(1):80–86. doi:10.1016/j.dental.2008.04.012
14. Park IS, Woo TG, Jeon WY, Park HH, Lee MH, Bae TS, Seol KW (2007) Surface characteristics of titanium anodized in the four different types of electrolyte. Electrochim Acta 53(2):863–870. doi:10.1016/j.electacta.2007.07.067
15. Kumar S, Sankara Narayanan TSN, Sundara Raman SG, Seshadri SK (2010) Surface modification of CP-Ti to improve the fretting-corrosion resistance: thermal oxidation vs. anodizing. Mater Sci Eng C 30(6):921–927. doi:10.1016/j.msec.2010.03.024
16. Dong H, Bell T (1999) Designer surfaces for titanium components. Anti Corros Methods Mater 46(3):181–188. doi:10.1108/00035599910273160
17. Krupa D, Baszkiewicz J, Kozubowski JA, Barcz A, Sobczak JW, Biliński A, Lewandowska-Szumieł M, Rajchel B (2002) Effect of phosphorus-ion implantation on the corrosion resistance and biocompatibility of titanium. Biomaterials 23(16):3329–3340. doi:10.1016/S0142-9612(02)00020-0
18. Krupa D, Baszkiewicz J, Kozubowski J, Barcz A, Sobczak J, Biliński A, Rajchel B (2001) The influence of calcium and/or phosphorus ion implantation on the structure and corrosion resistance of titanium. Vacuum 63(4):715–719. doi:10.1016/S0042-207X(01)00263-9
19. Xie Y, Liu X, Huang A, Ding C, Chu PK (2005) Improvement of surface bioactivity on titanium by water and hydrogen plasma immersion ion implantation. Biomaterials 26(31):6129–6135. doi:10.1016/j.biomaterials.2005.03.032
20. Zhecheva A, Malinov S, Sha W (2006) Titanium alloys after surface gas nitriding. Surf Coat Technol 201(6):2467–2474. doi:10.1016/j.surfcoat.2006.04.019
21. Boettcher C (2000) Deep case hardening of titanium alloys with oxygen. Surf Eng 16(2):148–152. doi:10.1179/026708400101517053
22. Qi P-Y, Li XY, Dong H, Bell T (2002) Characterisation of the palladium-modified thermal oxidation-treated titanium. Mater Sci Eng A 326(2):330–342. doi:10.1016/S0921-5093(01)01701-4
23. Omidbakhsh F, Ebrahimi AR (2016) Lattice parameters of Ti-4Al-2V alloy with thermal oxidation. Rare Metals 35(2):149–153. doi:10.1007/s12598-015-0452-2
24. Aniołek K, Kupka M, Barylski A, Dercz G (2015) Mechanical and tribological properties of oxide layers obtained on titanium in the thermal oxidation process. Appl Surf Sci 357(Part B):1419–1426. doi:10.1016/j.apsusc.2015.09.245
25. Wen M, Wen C, Hodgson P, Li Y (2014) Improvement of the biomedical properties of titanium using SMAT and thermal oxidation. Coll Surf B Biointerfaces 116:658–665. doi:10.1016/j.colsurfb.2013.10.039
26. Durante M, Boccarusso L, Velotti C, Astarita A, Squillace A, Carrino L (2016) Characterization of Ti-6Al-4V tribopairs: effect of thermal oxidation treatment. J Mater Eng Perform 26(2):571–583. doi:10.1007/s11665-016-2477-6
27. Karlsson P, Krahmalev P, Gåård A, Bergström J (2013) Influence of work material proof stress and tool steel microstructure on galling initiation and critical contact pressure. Tribol Int 60:104–110. doi:10.1016/j.triboint.2012.10.023
28. Andreasen JL, Bay N, De Chiffre L (1998) Quantification of galling in sheet metal forming by surface topography characterisation. Int J Mach Tools Manuf 38(5–6):503–510. doi:10.1016/S0890-6955(97)00095-3
29. Wiklund U, Hutchings IM (2001) Investigation of surface treatments for galling protection of titanium alloys. Wear 251(1–12):1034–1041. doi:10.1016/S0043-1648(01)00730-X
30. Donachie MJ (2000) Titanium: a technical guide, 2nd edn. International, ASM
31. Formisano A, Boccarusso L, Carrino L, Durante M, Langella A, Memola Capece Minutolo F, Squillace A (2016) Formability and surface quality of incrementally formed grade 1 titanium thin sheets. Key Eng Mater 716:99–106. doi:10.4028/www.scientific.net/KEM.716.99
32. Behera AK, Ou H (2016) Effect of stress relieving heat treatment on surface topography and dimensional accuracy of incrementally formed grade 1 titanium sheet parts. Int J Adv Manuf Technol 87(9):3233–3248. doi:10.1007/s00170-016-8610-8
33. Hussain G, Gao L, Zhang ZY (2008) Formability evaluation of a pure titanium sheet in the cold incremental forming process. Int J Adv Manuf Tech 37:920–926. doi:10.1007/s00170-007-1043-7
34. Formisano A, Astarita A, Boccarusso L, Capece Minutolo F, Carrino L, Durante M, Langella A, Squillace A (2015) Formability evaluation of grade 1 titanium sheets depending on the temperature by FE analyses. Key Eng Mater 651-653:1054–1059. doi:10.4028/www.scientific.net/KEM.651-653.1054
35. Chen F-K, Chiu K-H (2005) Stamping formability of pure titanium sheets. J Mater Process Tech 170(1–2):181–186. doi:10.1016/j.jmatprotec.2005.05.004
36. Astarita A, Durante M, Langella A, Squillace A (2013) Elevation of tribological properties of alloy Ti – 6% Al – 4% V upon formation of a rutile layer on the surface. Met Sci Heat Treat 54(11–12):662–666. doi:10.1007/s11041-013-9567-y
37. Durante M, Formisano A, Langella A, Memola Capece Minutolo F (2009) The influence of tool rotation on an incremental forming process. J Mater Process Tech 209(9):4621–4626. doi:10.1016/j.jmatprotec.2008.11.028
38. Capece Minutolo F, Durante M, Formisano A, Langella A (2007) Evaluation of the maximum slope angle of simple geometries carried out by incremental forming process. J Mater Process Tech 194(1–3):145–150. doi:10.1016/j.jmatprotec.2007.04.109
39. Lu B, Fang Y, Xu DK, Chen J, Ou H, Moser NH, Cao J (2014) Mechanism investigation of friction-related effects in single point incremental forming using a developed oblique roller-ball tool. Int J Mach Tools Manuf 85:14–29. doi:10.1016/j.ijmachtools.2014.04.007